



Standardization of Shape Memory Alloys from Material to Actuator

D. E. Nicholson¹ · O. Benafan² · G. S. Bigelow² · D. Pick³ · A. Demblon⁴ · J. H. Mabe⁴ · I. Karaman⁴ · B. Van Doren⁵ · D. Forbes⁶ · F. Sczerzenie⁷ · L. Fumagalli⁸ · C. Wallner⁹

Received: 26 January 2023 / Accepted: 23 February 2023 / Published online: 28 March 2023
© ASM International 2023

Abstract Development of standard specifications and test methods for shape memory alloys (SMAs) in the context of actuator materials and components are outlined. A material specification centers on mill product wrought NiTi or NiTi + X + X' based alloys, where X and X' can be any alloying element addition to the base NiTi. This standard is aimed toward specifying the chemical, mechanical, thermal, and metallurgical requirements of NiTi-based alloys. Two newly proposed standard test methods are aimed toward expanding the applicability of the following published SMA actuator standards: E3097—Standard Test Method for Uniaxial Constant Force Thermal Cycling (UCFTC) and E3098—Standard Test Method for Uniaxial Pre-strain and Thermal Free Recovery (UPFR). First, Force-Controlled Repeated Thermal Cycling (FCRTC), addresses repeated thermal cycling under a constant force and associated terminology. FCRTC's primary objective is

to address failure with regard to the SMA material's ability to perform its function as an actuator for an application's required lifecycle. Second, Constant Torque Thermal Cycling (CTTC) deals with thermally cycling SMAs under a constant torque for rotary actuator applications. Key features of each proposed standard and progress on their development are outlined, considering novelty and applicability to actuation from raw material to final actuator component in its application.

Keywords Shape memory alloy · Actuation · ASTM · Standards · Specifications · Fatigue · Torsion

Introduction

Shape memory alloy (SMA) based actuators are currently used for many commercial applications across several industries, including medical, consumer goods, automotive, and space exploration [1]. With the capability of generating large forces and doing significant work in a very robust, energy-dense, and compact design, SMAs provide a high-value actuation technology for a broad range of aeronautical applications as well [2–7]. Despite these proven benefits, their transition from prototype demonstration to commercial use in flight-critical aeronautical applications has not reached full potential. One of the primary identified needs limiting full-scale commercial use of SMA actuations in the commercial aviation industry is a lack of accepted industry and regulatory testing and certification standards [4, 8]. The Federal Aviation Administration (FAA), with a mission to provide the safest, most efficient aerospace system in the world, establishes some of the highest requirements of any industry for entry into commercial use. Guidance is provided under the U.S. Code of

✉ D. E. Nicholson
douglas.e.nicholson@boeing.com

¹ The Boeing Company, Berkeley, MO 63134, USA

² Materials and Structures Division, NASA Glenn Research Center, Cleveland, OH 44135, USA

³ Kinitics Automation Limited, Vancouver, BC V5X 0A4, Canada

⁴ Department of Materials Science and Engineering, Texas A&M University, College Station, TX 77843, USA

⁵ ATI Specialty Alloys and Components, Albany, OR 97321, USA

⁶ Fort Wayne Metals, Fort Wayne, IN 46809, USA

⁷ SAES Smart Materials, New Hartford, NY 13413, USA

⁸ SAES Getters S.p.A, 20045 Lainate, MI, Italy

⁹ Embraer, São José dos Campos 12227-901, Brazil

Federal Regulations (CFR) for the establishment of airworthiness certification for materials (Title 14, Part 25), which states: *the suitability and durability of materials used for parts, the failure of which could adversely affect safety, must be established on the basis of experience or tests; conform to approved specifications that ensure their having the strength and other properties assumed in the design data; and take into account the effects of environmental conditions, such as temperature and humidity, expected in service (Part 25.603).*

To conform to these regulations, standard material specifications and test methods must be established. Such standards are needed to support model parametrization, development of design allowables, supplier qualification, and regulatory approval of SMA materials and components for actuation. Industries outside of the aerospace field and non-flight-critical applications have seen successful commercial use of SMA actuation without such standards by relying on internal qualification procedures or, in some cases, standards for superelastic SMAs developed primarily for medical applications [9–14]. These other industries could experience more widespread use of SMA applications with optimized manufacturing processes and quality assurance guided by standards developed specifically for actuation.

With these needs in mind, a committee was formed under the Aerospace Vehicle Systems Institute (AVSI) with members from industry, government, and academia to develop and publish standard test methods that are specifically intended to measure SMA actuation properties. Under this committee, standard test methods for Uniaxial Constant Force Thermal Cycling (UCFTC) and Uniaxial Pre-strain and Thermal Free Recovery (UPFR) were published under ASTM as E3097 and E3098, respectively [15, 16]. These two test methods capture the two most important responses in SMAs for actuation: load-biased shape memory effect and classical shape memory effect. These test methods measure transformation properties such as transformation temperature, actuation strain, and residual strain to provide data for the characterization and selection of SMA materials, quality control, design allowables, and actuator design. Since their publication in 2017, E3097 and E3098 are beginning to see more widespread use in industry and academia. Commensurate with this effort, supporting method evaluations and analysis tools were developed to aid their adoption. The ruggedness evaluation of both test methods [17] was conducted to assess the sensitivity of these methods and ensuing significances. These studies highlight key factors that could influence test results, and they provide a representative practice of the test methods. Data extraction tools have also been developed to extract and analyze raw data generated by the test methods and to output all required results

[18, 19]. Additionally, an interlaboratory study (ILS) is ongoing to determine the precision of test methods E3097 and E3098.

A material specification and additional test methods are still needed to fully support the use of SMA actuators in commercial applications. First, a material specification is needed that establishes requirements and acceptance test methods to control the wrought material. Second, there is a recognized need for a test method that defines and evaluates the evolution of actuation properties and actuation lifecycle during repeated UCFTC. Third, rotary SMA actuation has been demonstrated as a practical and valuable actuator form, as highlighted recently during flight test of the spanwise adaptive wing, reconfigurable vortex generators, and actuated wind tunnel models [4–7]. To this end, a material specification and two new test methods have been proposed to ASTM that extend the applicability of E3097 to repeated UCFTC and torsional testing [20–22]. With the two published test methods and the proposed material specification and test methods, the overall objective is to provide a suite of SMA standards for actuation that evaluate and control the alloy from raw material to final actuator component in its application.

To manage this broader effort, an ASTM task group (E08.05.10—Shape Memory Alloys for Actuation), in association with the Consortium for the Advancement of Shape Memory Alloy Research and Technology (CAS-MART) and AVSI, was formed to develop standards for characterizing the thermomechanical behavior and material properties of SMAs subject to thermally induced phase change. Material specifications and test methods developed under this task group support SMA material evaluation and actuator design, including the effect of thermomechanical cycling on the material and shape memory effect properties. Figure 1 shows the ecosystem and process flow for the current and in-work material specifications and test methods for SMAs for actuation being maintained and developed under E08.05.10. While it is not the focus of the current paper, processing can also significantly affect the actuator performance of SMA material and is the subject of many works [23–27]. Under the proposed framework, future internal and published standards may be developed that address forming and post-processing (including heat treatment, annealing, shape setting, extruding, machining, and training) into semifinished and finished components such as sheet, bar, wire, and tube. Future test methods addressing fracture toughness of SMA materials under actuation relevant loading conditions will also be needed [28]. This paper will provide an update on the development of SMA standard specifications and test methods for actuator applications, highlighting their need, background, and envisioned approaches while providing some guidance on their use.

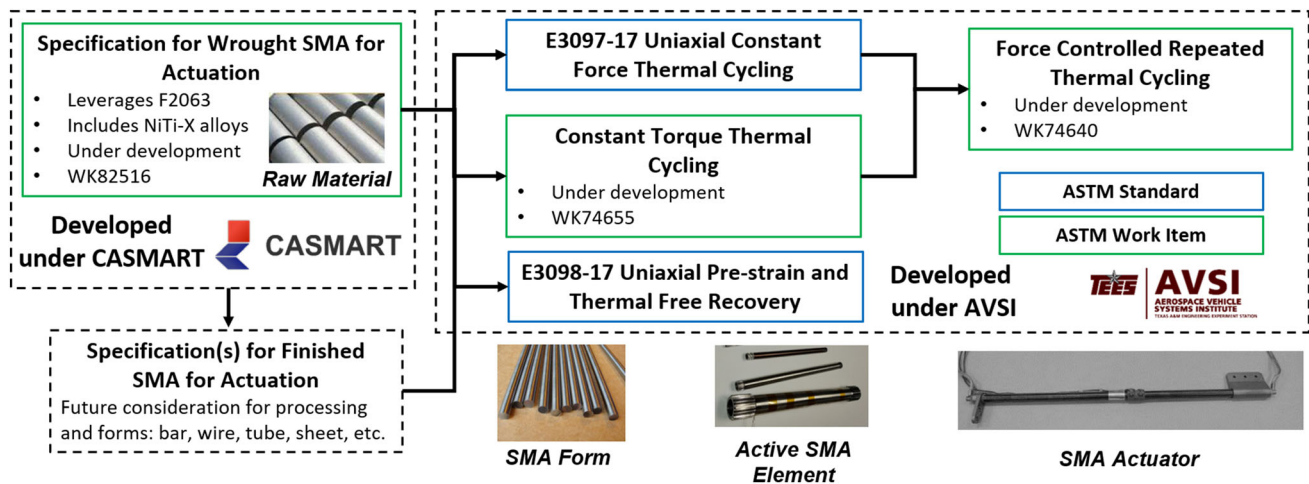


Fig. 1 Ecosystem and process flow for the current and in-work material specifications and test methods for SMAs for actuation being maintained and developed under E08.05.10

Standard Material Specification for SMAs for Actuation

Several thousand NiTi-based SMA systems have been systematically evaluated for actuation properties, and the data are now compiled in an interactive database [29, 30]. Many of these renewed NiTi-X (e.g., X = Hf, Pt, Pd, Au, Zr) SMA alloys have properties that have been optimized for actuation, including improved dimensional stability and tailored transformation temperatures. However, to date only one SMA system is currently controlled by a standard material specification: binary NiTi with 54.5 to 57.0 wt% Ni as specified by the F2063 standard, which focuses primarily on wrought NiTi used for superelastic medical devices and applications. In addition to composition, it is also established from prior works that impurities, non-metallic inclusions, dislocations, etc., significantly affect actuation performance and fatigue life, but most of these new alloys have only been produced in experimental quantities and do not necessarily comply with or fit the F2063 scope. These shortcomings form the basis for developing new specifications directly applicable to NiTi-based SMAs suited for actuation purposes.

Starting with the case of NiTiHf alloys, compositions with nominal 45 wt% Hf content have been globally studied with regard to thermophysical properties [31], thermal properties, processing maps [27], actuation properties and, more recently, fatigue properties [32]. All of these findings are in part reliant on the starting ingot, which differs from one study to the next. Preceding these Hf alloys are the NiTi-Cu, NiTi-Nb, and NiTi-Pt alloys, along with the succeeding NiTi-Zr-based alloys, which follow an analogous developmental outline. Nonetheless, they all lack a guidance document to specify the mill product. The intent of the proposed “specification for wrought NiTi-

based shape memory alloys for actuation” described herein is to specify such recommendations and guidance for the chemical, physical, mechanical, thermal, and metallurgical requirements for wrought NiTi-based systems used for actuation.

One of the major deviations from F2063 in the proposed specification is the revised designation of certain “residual elements” as “alloying elements,” given their role in achieving the desired actuation properties. For instance, Fe and Cu elements are considered residual elements in F2063 and are limited to < 500 ppm for wrought NiTi specifications, but these same elements can be used in much higher percentages as the elemental additions to form ternary or higher order alloying compounds for actuation purposes. Other elements, such as carbon, oxygen, nitrogen, and hydrogen, are still considered residual elements in the proposed specification that would be subject to the maximum content limits. Table 1 provides an example of the chemical composition requirements for select alloys. Note, during alloy development, atomic percentage is often used to specify alloy composition. Therefore, common designations in literature will often carry indications of the alloy’s ternary element in at.% because this was the designation given to them at creation—for example, NiTiHf₂₀ (with 20 at.% or 45 wt% Hf). However, it is more practical for commercial material suppliers to use wt%, therefore the material specification and examples in Table 1 specify the alloy composition in wt%.

Residual elements covered under this specification are controlled to certain limits to ensure good shape memory properties. The most significant residual elements are carbon (< 0.050 wt%), oxygen (< 0.050 wt%), and hydrogen (0.005 wt%). These elements can form non-metallic inclusions (e.g., carbides or oxides) that cause major deficiencies in SMA actuators in the final product form. An

Table 1 An example of chemical composition requirements under consideration for the new specification for wrought NiTi-based SMAs for actuation

Designation	Grade	Nickel range or balance	Titanium range or balance	Cobalt	Chromium	Niobium	Copper	Niobium	Iron	Hafnium	Zirconium	Gold	Platinum	Palladium
NiTi (F2063)	-	54.5 to 57.0	Balance	0.05 max	0.010 max	0.025 max	0.010 max	0.025 max	0.050 max	-	-	-	-	-
NiTi (reserved)	-	54.0 to 60.0	Balance	-	-	-	-	-	-	-	-	-	-	-
NiTiHf-20	-	36.0 to 37.7	Balance	-	-	-	-	-	-	45 ± 0.1	1.0 max	-	-	-
NiTiZr-20	-	46.5 to 48.3	Balance	-	-	-	-	-	-	1.0 max	29.4 ± 0.1	-	-	-
NiTiPd-20	-	27.1 to 29.0	Balance	-	-	-	-	-	-	-	-	-	-	33.85 ± 0.1
NiTiCu-15	-	38.0 to 39.0	Balance	-	-	-	17.65	-	-	-	-	-	-	-
NiTiFe-2	-	52.0 to 53.0	Balance	-	-	-	-	-	2 ± 0.1	-	-	-	-	-
NiTi-X	-	Ni content	Balance	X	X = Any element	X	X	X	X	X	X	X	X	X

interesting aspect of the new specification are the provisions made for material grades that permit greater or lesser restrictive limits on residual content and material transformation temperatures. Such provisions allow for the specification to be broadly applicable in the field of actuation, where customer requirements for material performance vary in stringency. A flexible specification format also permits the addition of other material grades as both the state of the art and customer demands evolve. Grade designations are currently being considered for identifying the new and evolving set of NiTi-X alloy systems, as indicated by the “reserved” column in Table 1.

It is worth noting that this specification does not bound a range of Ni content to binary alloy compositions, given such percentages change depending on the atomic site preference behavior. For instance, in the well-documented NiTi-Hf alloy, the Hf substitutes for Ti, whereas in the NiTi-Pd alloys, the Pd substitutes for Ni. Hence a general specification on Ni percentages is not pursued in this specification, but rather the entire compositional description is designated. Another major deviation from F2063 are the additional limits placed on transformation temperatures beyond the austenitic start temperature that is specified in the medical standard. As the application of SMAs for actuation typically involves thermal cycling of the material to induce the shape memory effect, the presence of hysteresis in the thermomechanical behavior of NiTi-based SMAs is relevant to the performance and behavior of an SMA actuator. Martensitic finish temperature, for example, heavily influences the upper operating temperature limit of the final actuator, hence one of the key additions of the specification is that it allows for ternary high-temperature SMA (HTSMA) systems (e.g., NiTiHf) to be specified.

Force-Controlled Repeated Thermal Cycling (FCRTC)

The first thermal cycle in Fig. 2a highlights UCFTC, in which a SMA specimen is heated to the upper cycle temperature (UCT) under no-load, loaded to a prescribed stress value, then cooled to the lower cycle temperature (LCT) and heated to the UCT, maintaining constant force. For each thermal cycle under load, key strain metrics are indicated, including the initial loading strain (e_i), strain at the UCT (e_{UCT}), strain at the LCT (e_{LCT}), actuation strain ($e_{act} = e_{LCT} - e_{UCT}$), and residual strain ($e_{res} = e_{UCT} - e_i$). These strain metrics can then be plotted as a function of cycle number to illustrate how these values evolve throughout the lifetime of the material (Fig. 2b). When SMAs undergo UCFTC, the repeated phase transformation generates material defects, resulting in the accumulation of residual strain, as evidenced in Fig. 2b. Residual strain

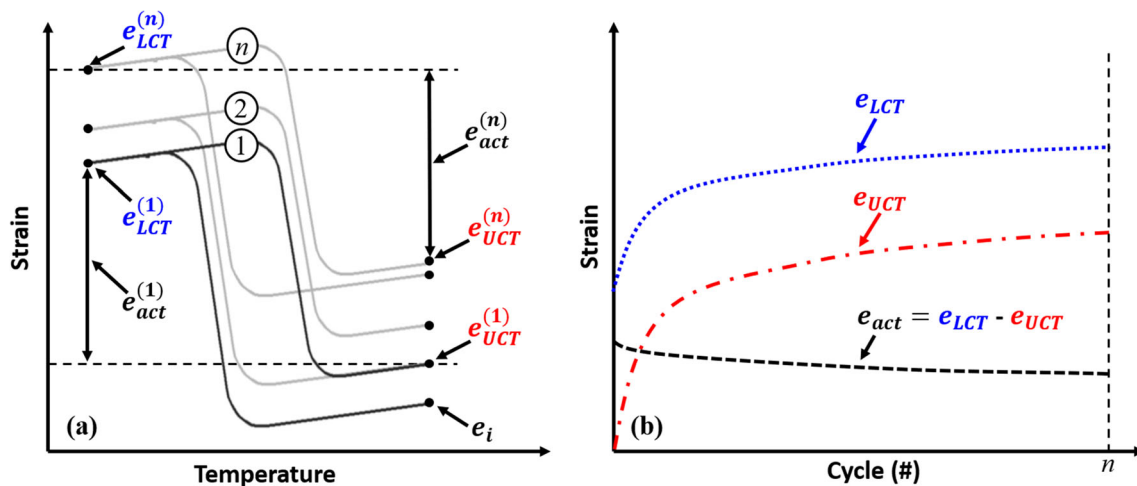


Fig. 2 Force-Controlled Repeated Thermal Cycling (FCRTC) of shape memory alloys. **a** Typical strain-temperature response under constant force, **b** pointwise strain data as a function of cycle number corresponding to strain in the UCT, LCT, and the calculated actuation strain

accumulation is undesirable, as it promotes both functional and structural fatigue. This is not to be confused with conventional material fatigue and failure due to fracture under a fluctuating load. The objective here is to address failure with regard to the SMA material's ability to perform in an actuation application for the application's required lifecycle.

The evolutionary behavior has been referred to by many names within the SMA community, such as dimensional stability, ratcheting, transformation-induced plasticity (TRIP), and functional and actuation fatigue. SMA fatigue can also cause an evolution in transformation temperatures and hysteresis as a function of thermal cycling, which can lead to shifts in transformation temperatures outside of the intended actuator use. The microstructural mechanisms governing this behavior (including dislocation-based plasticity, retained martensite, deformation twinning, variant interface motion, and phase boundary incompatibility) are difficult to decouple from thermoelastic recoverable mechanisms (including martensite reorientation/detwinning and phase transformation). While the mechanisms governing this behavior are the subject of many works, this effort seeks to develop a standard test method for quantifying the behavior for actuator applications regardless of the mechanisms causing it, and to define common terminology for describing it.

Numerous factors affect the actuation behavior of SMAs, including the material properties of the specific alloy under investigation. The effects of composition [33–35], precipitation [36, 37], non-metallic inclusions [38], and grain size [39, 40] have been studied across multiple SMA systems. The degree to which these material properties affect fatigue can vary among SMA systems but are influential regardless. Material performance enhancement is possible by optimizing these alloy properties

through careful control of the manufacturing and processing. However, seemingly small variations can result in large differences in transformation characteristics, as evidenced by the NiTiHf system, where deviations in Ni content of only 0.1 at.% can result in a shift in transformation temperatures up to 50 K [41]. In NiTi-based SMAs, minimizing non-metallic inclusions is also challenging due to the high affinity to oxygen of Ti. Additionally, reducing grain size and work hardening is difficult, as many SMAs have a low workability. These factors are further compounded by different manufacturing methods and melt scale-up [27]. It is inevitable that the actual composition will differ from the nominal composition, and improving the repeatability in manufacturing SMAs is an ongoing effort. As an example, Fig. 3 illustrates how these differences in materials with the same nominal composition lead to drastically different fatigue behavior [33]. In this study, four lots of material with the same nominal composition (Ni_{50.3}Ti_{29.7}Hf₂₀ at.%) were investigated; each lot had been produced in the same manner by the same manufacturer. From the figure, it is clearly seen how varied the actuation strain response (e_{act}) is across all four materials, resulting in different magnitudes and evolution of actuation strain. This reiterates the importance of developing the standard for the production and reporting of wrought NiTi-based alloys, as discussed in “Standard Material Specification for SMAs for Actuation” section.

Beyond the effects of material properties, SMA implementation and test conditions can also significantly alter the fatigue response. A variety of studies have shown how several factors can influence the observed actuation performance, with the most prominent factors being degree of transformation [42–47], heating and cooling rate [42, 48], applied load [36], and UCT [49, 50]. To demonstrate the significance of test parameters, Fig. 4 shows the evolution

of actuation strain (e_{act}) during FCRTC for samples of the same material tested under the same conditions with the exception of UCT, which varied. There is a clear variation in fatigue response with higher UCTs, resulting in higher sustained actuation strains at the expense of fatigue life. Lower UCTs yielded longer lifetimes with a reduced magnitude and greater attenuation in actuation strain as a function of the number of cycles to failure. Where conventional materials may be less affected by relatively small variations, the added complexity associated with phase transformation amplifies the significance of such factors.

With all of this in mind, a standard test method for Force-Controlled Repeated Thermal Cycling (FCRTC) of SMAs is being developed with ASTM under the E08.05.10 subcommittee [21]. Preliminary considerations for FCRTC are specimen geometries, test apparatus, extensometry, heating/cooling methods, LCT, UCT, and test results (outputs, e.g., transformation strains and temperatures) as defined in E3097. Additional test results will include (but are not limited to) a quantification of stability as it relates to accumulated residual strain and the derivative of the strain-cycle profiles shown in Fig. 2b. Test control parameters, including LCT, UCT, stress value, and stop condition, will be defined by the program or user. LCT, UCT, and force (corresponding to the set stress value) will remain constant throughout the duration of the test. The specimen will be cycled until it meets a specified stop condition: (1) an actuation property (e.g., stability or minimum actuation strain); (2) failure, crack, or rupture; (3) maximum elongation; (4) number of cycles (n); or 5) program/user defined. Typically, actuation fatigue comprises functional fatigue and structural fatigue. Functional fatigue relates to the deterioration of the degree of transformation (indicated by reduced actuation strain) with

repeated thermal cycling under load, which could be a type (1) stop condition as described in the preceding list. Structural fatigue relates to the number of cycles until failure due to fracture, which would apply to a type (2) stop condition. The addition of stop conditions (3), (4), and (5) is more applicable to actuator-specific type testing, where design constraints require alternative constraints to be met. Note that FCRTC performed with stop condition (1) could also describe a typical SMA training routine via actuation cycling.

The proposed test method captures a very common test that has already been utilized in many studies; binary NiTi [32, 51], NiTi-Cu [52], NiTi-Hf [33, 36], NiTi-Zr [53], NiTi-Pd [54] were among the many SMA systems studied. Versions of this procedure were also used to test various forms, such as flat bars [36], round dog bones, wires [55], and springs [52]. In cases where a similar alloy was tested by dissimilar test houses or groups, differing results can be attributed to the lack of a unified testing method. In the absence of such a method, the executed test protocols, nomenclature, and reporting are different, thus emphasizing the need for a standardized methodology. Additionally, the same materials tested were sourced from different vendors, without a uniform specification on impurities, inclusion, or relevant tolerances. Hence, differences from test to test are also expected without a standardized material specification.

Constant Torque Thermal Cycling (CTTC)

Torsional SMA rotary actuators offer a valuable actuation mode for many aeronautical applications that require discrete ranged rotary motion, including aircraft control surfaces [4, 56]. This form and actuation mode often use the

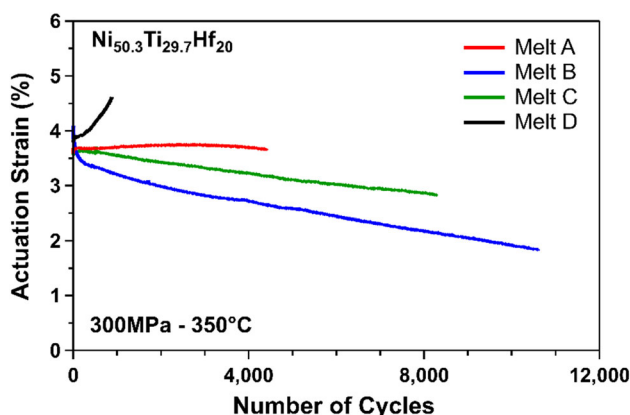


Fig. 3 Actuation strain evolution comparison of four separate batches of material with the same nominal composition of $\text{Ni}_{50.3}\text{Ti}_{29.7}\text{Hf}_{20}$ (at.%). The batches were manufactured in the same manner by the same supplier, but variations in actual composition, impurities, and grain size resulted in significantly different actuation responses

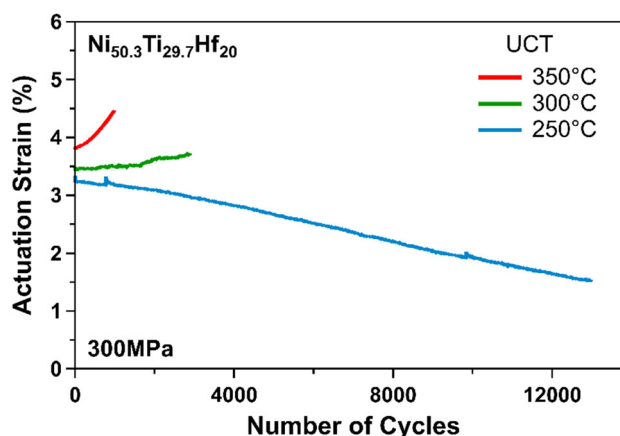


Fig. 4 Actuation strain evolution comparison of a single $\text{Ni}_{50.3}\text{Ti}_{29.7}\text{Hf}_{20}$ (at.%) material tested under the same conditions with the exception of upper cycle temperature (UCT), which varied

SMA's high energy density by providing the ability to integrate the SMA rotary actuator directly into the hinge line. This reduces the need for complex kinematics, linkages, etc., required to transmit the work output of the actuator. Recent examples have demonstrated rotary SMA actuation as a practical and valuable actuator form during flight test of the adaptive trailing edge (ATE), spanwise adaptive wing (SAW), reconfigurable vortex generators (SMART-VG), and actuated wind tunnel models [4–7]. The torsional stress state in a thin-walled tube is fairly homogenous, thus activation of the material and work output per unit mass is nearly that of a uniaxial wire- or bar-based SMA actuator. Furthermore, when a SMA cylindrical specimen undergoes large torsional deformations, cross-sectional area geometry change is typically negligible. Therefore, unlike wire or springs under axial deformation or beams under bending, the cross-sectional geometry does not significantly change with strain evolution observed during repeated thermal cycling. Aeronautical applications often require actuation against external loads in multiple directions. Applications that require actuation against bidirectional (clockwise or counter-clockwise) loading include flight control devices such as trailing edge wing-flap actuators, where actuation above and below a faired position creates hinge-line torques in two directions. Due to its ability to function bidirectionally, an SMA rotary actuator can also develop two-way shape memory effect (TWSME) that is beneficial in these applications. Training of SMA by repeated constant-torque thermal cycling has been shown to produce stable TWSME in SMA rotary actuators, which reduces the need for an external bias force or antagonistic SMA elements [57–59].

With these benefits and promising applications in mind, a standard test method for Constant Torque Thermal Cycling (CTTC) of cylindrical SMA specimens is being developed under ASTM [22]. This test method will measure transformation properties such as transformation temperatures, actuation strain, TWSME strains, and residual strains in cylindrical SMA tube components under torsional loading. Preliminary considerations for CTTC include test apparatus, control modes, shear stress, and shear strain, which will be determined in accordance with E2207 (Standard Practice for Strain-Controlled Axial–Torsional Fatigue Testing with Thin-Walled Tubular Specimens). Here rotation (θ) and applied torque (T) are reported as shear strain and shear stress, respectively, calculated at the outer diameter (D) as follows: shear strain $\gamma = D\theta/(2L)$ and shear stress $\tau = 16TD/[\pi(D^4 - d^4)]$, where L is gauge length and d is the inner diameter. Note that during CTTC and torsional loading of cylindrical SMA specimens, shear strain typically varies non-linearly through the wall of the specimen, with the smallest and largest values occurring at the inner and outer diameters of

the specimen, respectively [60, 61]. Also, CTTC anticipates allowing for specimens that do not meet the thin-walled condition. Therefore, shear strain and shear stress results determined on the outer diameter will be considered representative of specimens of the NiTi-based material and outer-to-inner-diameter ratio being tested. Heating/cooling methods, LCT, UCT, and test results will be similar to E3097 with consideration of test-direction-specific nomenclature such as shear strain (γ) and actuation shear strain (γ_{act}).

The baseline control mode will be axially free CTTC, in which a thermal cycle is performed in torque control under constant torque with no axial loading or axial loads not exceeding a fixed minimal value. Specimen geometry will be limited to circular cross-sections, and end-connections will be required to maintain torsional compliance throughout the test. Examples of splined and hexed end-connections and grips used to maintain torsional compliance are shown in Ref. [57, 58] and [7], respectively. Ref. [58] shows an example of non-contact extensometry used during thermomechanical cycling of SMA torsional specimens to acquire shear strain data. For wires and specimens in component form, angular displacement may be measured between the grips and shear strain shall be determined in accordance with E2207 on the outer diameter. Figure 5 shows an example of a test rig designed for training and characterizing SMA tube components under CTTC. Figure 5a shows a test rig with a pulley used to transmit dead load at the end of a SMA tube component with a rotating and fixed end. The tube was fabricated from near-equiatomic binary NiTi produced to F2063 and was tested in its as-annealed state. Splined end-connections and corresponding grips are used to maintain torsional compliance between the fixed and rotating ends of the tube throughout the test, as shown in Fig. 5b. Shear strain and stress are calculated at the tube end-connections from angular displacement and torque measured at the grips. Shear strain and shear stress were calculated in accordance with E2207. Heating was performed using an internal cartridge heater, and the tube was allowed to cool convectively. The LCT and UCT were selected and maintained in accordance with E3097. This setup provides an example of a simple test rig that can potentially perform CTTC on a specimen in component form without the need for an axial-torsion load frame described in E2207. This setup is similar to the test rig used in Ref. [57, 59]. More details on the material and tube geometry can be found in Ref. [59].

To demonstrate CTTC, the specimen was (1) heated to a UCT = 140 °C under no-load condition; (2) torqued to generate an equivalent shear stress of $\tau = 138$ MPa (20 ksi), and from this point on torque was held constant; (3) cooled to an LCT = 30 °C; and (4) heated back to the UCT = 140 °C, as shown in Fig. 5c. Note that the shear

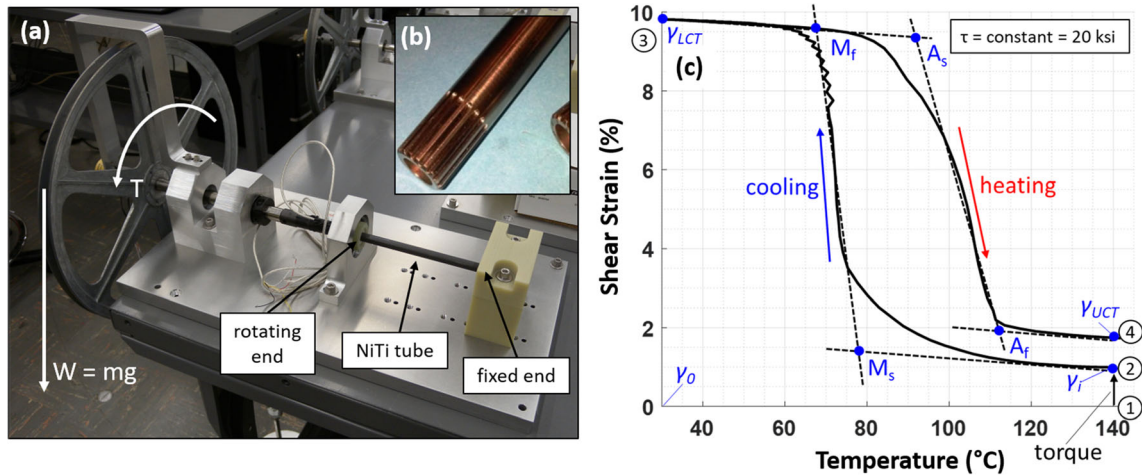


Fig. 5 Example of constant torque thermal cycling (CTTC) of a near-equiatomic binary NiTi tube component. **a** Constant torque test rig, **b** splined end-connections on tube, and **c** shear strain-temperature response

strain-temperature response generated from CTTC is graphically similar to the response generated by UCFTC performed in accordance with E3097, substituting strain and stress with shear strain and shear stress. This allows for extraction of test results and tangent fit methods from E3097 to be applied directly to the data generated by CTTC. Here, test results similar to E3097 are indicated and determined with torsion-specific nomenclature for shear strain (γ) at initial loading (γ_i) = 1.0%, LCT (γ_{LCT}) = 9.8%, and UCT (γ_{UCT}) = 1.7%. Actuation ($\gamma_{act} = \gamma_{UCT} - \gamma_{LCT}$) and residual ($\gamma_{res} = \gamma_{UCT} - \gamma_i$) shear strain are calculated to be 8.1% and 0.7%, respectively. The transformation temperatures martensite start (M_s), martensite finish (M_f), austenite start (A_s), and austenite finish (A_f)

were determined graphically by tangent fit to be 78 °C, 68 °C, 92 °C and 112 °C, respectively.

Another example of performing a CTTC test is using an axial-torsional servo-hydraulic load frame. These test machines provide additional controls and flexibility depending on the test program. Figure 6 shows an example NiTiHf torque tube with a splined end-connection that was tested under an applied shear stress of 100 MPa. Heating was performed using an induction coil wrapped around the tube and the gripping device to maintain a uniform temperature along the sample. For strain measurements, a digital image correlation (DIC) optical metrology system was used with a virtual strain gauge at the middle of the tube, as shown in Fig. 6b. In this experiment, the axial load

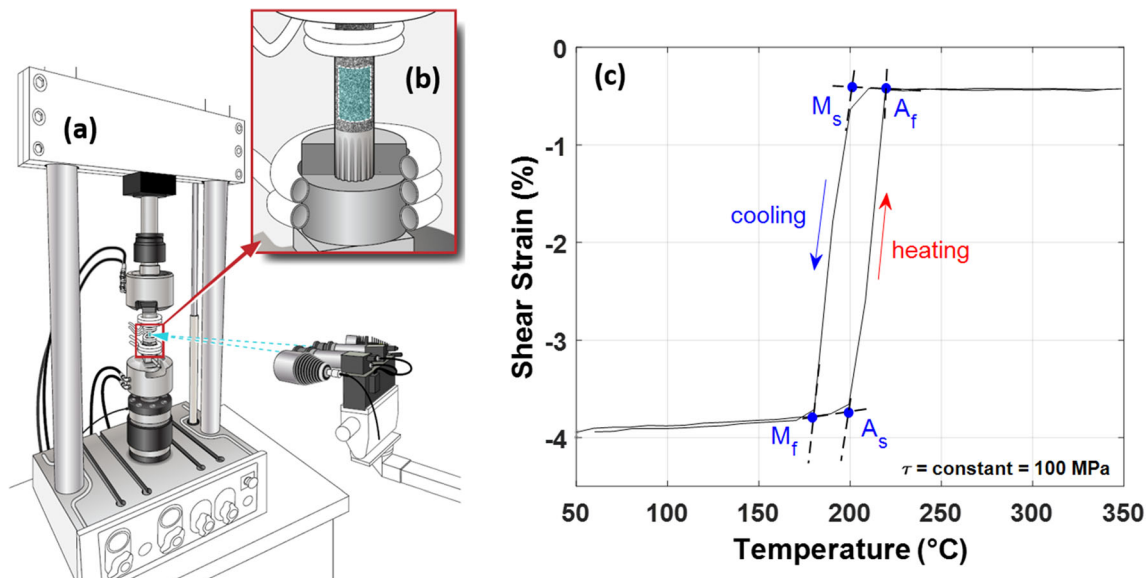


Fig. 6 Example of constant-torque thermal cycling (CTTC) of a ternary NiTiHf tube component. **a** Servo-hydraulic test rig [58] © 2018 IOP Publishing Ltd., **b** splined end-connections on tube and induction coils, and **c** shear strain-temperature response

was controlled to 0 N throughout the test. The resulting strain-temperature response is shown in Fig. 6c.

While the test equipment examples provided here are commonly used to carry out a CTTC test, other techniques and metrologies can be used as long as the outlined test procedures are satisfied (e.g., gradients, control mode).

Conclusions

Standard material specifications and test methods for SMA material and components for actuator applications were reviewed, highlighting their need, background, and envisioned approaches while providing some guidance on their use. The following standard material specification and two new test methods currently under development for SMAs for actuation were discussed in detail:

- **Material Specification**—a material specification that defines physical, mechanical, thermal, and metallurgical requirements for mill product wrought NiTi or NiTi + X + X'-based alloys, where X and X' can be any alloying element addition to the base NiTi.
- **Force-Controlled Repeated Thermal Cycling (FCRTC)**—a test method that defines and evaluates evolution, fatigue, and failure of actuation properties and actuation lifecycle during repeated thermal cycling under constant force.
- **Constant-Torque Thermal Cycling (CTTC)**—a test method that evaluates torsional properties of cylindrical specimens during thermal cycling under a constant torque for rotary actuator applications.

These new standards under development, along with the related published standards E3907 and E3098, are currently being maintained and developed under ASTM task group E08.05.10—Shape Memory Alloys for Actuation. Next steps for the new standards under development include performing relevant testing to establish or confirm requirements, finalizing drafts, balloting, and publishing per ASTM guidelines. Future work may include the development of standard specifications and test methods that address forming and post-processing into semifinished and finished components; fracture toughness of SMA materials under actuation-relevant loading conditions; and other areas identified as needed by the community. Here the overall objective is to facilitate widespread use of SMA actuator applications with optimized manufacturing processes, quality assurance, application design, and qualifications guided by standards developed specifically for actuation.

Acknowledgements The authors gratefully acknowledge the Aerospace Vehicle Systems Institute (AVSI) and Consortium for the

Advancement of Shape Memory Alloy Research and Technology (CASMA) organizations and their many members who contributed countless in-kind and volunteer hours to these efforts! Furthermore, the authors would like to acknowledge ASTM and its E08 members for providing a platform for developing, review for consensus, publishing, and maintaining the standards discussed here. OB and GSB acknowledge support from the NASA Aeronautics Research Mission Directorate (ARMD) Transformational Tools and Technologies (TTT) project.

References

1. Jani JM, Leary M, Subic A, Gibson MA (2014) A review of shape memory alloy research, applications and opportunities. *Mater Des* 1980–2015(56):1078–1113
2. Hartl DJ, Lagoudas DC (2007) Aerospace applications of shape memory alloys. *Proc Inst Mech Eng G* 221(4):535–552
3. Calkins FT, Mabe JH (2010) Shape memory alloy based morphing aerostructures. *J Mech Des* 132:111012–111021
4. Benafan O, Moholt MR, Bass M, Mabe JH, Nicholson DE, Calkins FT (2019) Recent advancements in rotary shape memory alloy actuators for aeronautics. *Shape Mem Superelasticity* 5(4):415–428
5. Calkins FT, Mabe JH: Flight test of a shape memory alloy actuated adaptive trailing edge flap. In: ASME 2016 conference on smart materials, adaptive structures and intelligent systems (2016)
6. Calkins FT, Nicholson DE, Fassmann A, Vijgen P, Yeeles C, Benafan O et al (2022) Shape memory alloy actuated vortex generators: development and flight test. In: SMST2022. ASM International, pp. 6–8
7. Benafan O, Gaydosh DJ, Bigelow GS, Noebe RD, Calkins FT, Nicholson DE (2022) Shape memory alloy actuated vortex generators: alloy design. In: Shape memory and superelastic technology
8. Hartl DJ, Mabe JH, Benafan O, Coda A, Conduit B, Padan R, Van Doren B (2015) Standardization of shape memory alloy test methods toward certification of aerospace applications. *Smart Mater Struct* 24(8):082001
9. ASTM F2004-17 (2017) Standard test method for transformation temperature of nickel-titanium alloys by thermal analysis. ASTM International, West Conshohocken, 2017. www.astm.org
10. ASTM F2005-17 (2017) Standard terminology for nickel-titanium shape memory alloys. ASTM International, West Conshohocken, 2017. www.astm.org
11. ASTM F2063-18 (2018) Standard specification for wrought nickel-titanium shape memory alloys for medical devices and surgical implants. ASTM International, West Conshohocken, 2017. www.astm.org
12. ASTM F2082-16 (2016) Standard test method for determination of transformation temperature of nickel-titanium shape memory alloys by bend and free recovery. ASTM International, West Conshohocken, 2017. www.astm.org
13. ASTM F2516-18 (2018) Standard test method for tension testing of nickel-titanium superelastic materials. ASTM International, West Conshohocken, 2017. www.astm.org
14. ASTM F2633-18 (2018) Standard specification for wrought seamless nickel-titanium shape memory alloy tube for medical devices and surgical implants. ASTM International, West Conshohocken, 2017. www.astm.org
15. ASTM E3097-17 (2017) Standard test method for mechanical uniaxial constant force thermal cycling of shape memory alloys. ASTM International, West Conshohocken, 2017. www.astm.org

16. ASTM E3098-17 (2017) Standard test method for mechanical uniaxial pre-strain and thermal free recovery of shape memory alloys. ASTM International, West Conshohocken, 2017. www.astm.org
17. Luna H, Bigelow GS, Benafan O (2022) Ruggedness evaluation of ASTM international standard test methods for shape memory materials: E3098 Standard Test Method for Mechanical Uniaxial Pre-strain and Thermal Free Recovery of Shape Memory Alloys (No. NASA/TM-2022)
18. Bigelow GS, Benafan O, Toom ZD (2022) SMAAnalytics—an automated software for the analysis of shape memory alloy test data. In: SMST2022. ASM International, pp 55–56
19. Kuner MC, Karakalas AA, Lagoudas DC (2021) ASMADA—a tool for automatic analysis of shape memory alloy thermal cycling data under constant stress. *Smart Mater Struct* 30(12):125003
20. Nicholson DE, Benafan O, Bigelow GS, Sczerzenie F, Forbes D, Van Doren B, Mabe JH, Demblon A, Karaman I (2022) An overview of ASTM standard test methods for shape memory alloy actuation materials. In: SMST2022. ASM International (pp. 59–60)
21. ASTM Work Item (WK74640) New test method for load control thermomechanical actuation cycling of shape memory alloys. ASTM International, West Conshohocken. www.astm.org
22. ASTM Work Item (WK74655) Constant torque thermal cycling of shape memory alloys. ASTM International, West Conshohocken. www.astm.org
23. Frick CP, Ortega AM, Tyber J, Maksound AEM, Maier HJ, Liu Y, Gall K (2005) Thermal processing of polycrystalline NiTi shape memory alloys. *Mater Sci Eng A* 405(1–2):34–49
24. Sharma N, Kumar K, Kumar V (2018) Post-processing of NiTi alloys: Issues and challenges. *Powder Metall Met Ceram* 56(9):599–609
25. Lahoz R, Puértolas JA (2004) Training and two-way shape memory in NiTi alloys: influence on thermal parameters. *J Alloys Compd* 381(1–2):130–136
26. Atli KC, Karaman I, Noebe RD, Gaydos D (2013) The effect of training on two-way shape memory effect of binary NiTi and NiTi based ternary high temperature shape memory alloys. *Mater Sci Eng A* 560:653–666
27. Benafan O, Bigelow GS, Garg A, Noebe RD, Gaydos DJ, Rogers RB (2021) Processing and scalability of NiTiHf high-temperature shape memory alloys. *Shape Mem Superelasticity* 7(1):109–165
28. Haghgouyan B, Hayrettin C, Baxevanis T, Karaman I, Lagoudas DC (2019) Fracture toughness of NiTi—towards establishing standard test methods for phase transforming materials. *Acta Mater* 162:226–238
29. Benafan O, Bigelow GS, Young AW (2020) Shape memory materials database tool—a compendium of functional data for shape memory materials. *Adv Eng Mater* 22:1901370. <https://doi.org/10.1002/adem.201901370>
30. <https://shapememory.grc.nasa.gov>. Accessed Sept 2022
31. Keret-Klainer M, Padan R, Khoptiar Y et al (2022) Tailoring thermal and electrical conductivities of a Ni-Ti-Hf-based shape memory alloy by microstructure design. *J Mater Sci* 57:12107–12124. <https://doi.org/10.1007/s10853-022-07383-6>
32. Benafan O, Noebe RD, Padula SA II, Brown DW, Vogel S, Vaidyanathan R (2014) Thermomechanical cycling of a NiTi shape memory alloy—macroscopic response and microstructural evolution. *Int J Plast* 56:99–118
33. Demblon A, Karakoc O, Sam J, Zhao D, Atli KC, Mabe JH, Karaman I (2022) Compositional and microstructural sensitivity of the actuation fatigue response in NiTiHf high temperature shape memory alloys. *Mater Sci Eng A* 838:142786. <https://doi.org/10.1016/j.msea.2022.142786>
34. Frenzel J, George EP, Dlouhy A, Somsen C, Wagner M-X, Eggeler G (2010) Influence of Ni on martensitic phase transformations in NiTi shape memory alloys. *Acta Mater* 58(9):3444–3458
35. Frenzel J, Wiecezorek A, Opahle I, Maaß B, Drautz R, Eggeler G (2015) On the effect of alloy composition on martensite start temperatures and latent heats in Ni–Ti-based shape memory alloys. *Acta Mater* 90:213–231
36. Karakoc O, Hayrettin C, Evirgen A, Santamarta R, Canadinc D, Wheeler RW, Wang SJ, Lagoudas DC, Karaman I (2019) Role of microstructure on the actuation fatigue performance of Ni-Rich NiTiHf high temperature shape memory alloys. *Acta Mater* 175:107–120
37. Kreitzberg A, Brailovski V, Prokoshkin S, Facchinello Y, Inaekyan K, Dubinskiy S (2013) Microstructure and functional fatigue of nanostructured Ti–50.26at%Ni alloy after thermomechanical treatment with warm rolling and intermediate annealing. *Mater Sci Eng A*. <https://doi.org/10.1016/j.msea.2012.11.013>
38. Rahim M, Frenzel J, Frotscher M, Pfetzing-Micklich J, Steegmüller R, Wohlschlägel M, Mughrabi H, Eggeler G (2013) Impurity levels and fatigue lives of pseudoelastic NiTi shape memory alloys. *Acta Mater*. <https://doi.org/10.1016/j.actamat.2013.02.054>
39. LePage WS, Ahadi A, Lenthe WC, Sun QP, Pollock TM, Shaw JA, Daly SH (2018) Grain size effects on NiTi shape memory alloy fatigue crack growth. *J Mater Res*. <https://doi.org/10.1557/jmr.2017.395>
40. Yin H, He Y, Moumni Z, Sun Q (2016) Effects of grain size on tensile fatigue life of nanostructured NiTi shape memory alloy. *Int J Fatigue*. <https://doi.org/10.1016/j.ijfatigue.2016.03.023>
41. Umale T, Salas D, Tomes B, Arroyave R, Karaman I (2019) The effects of wide range of compositional changes on the martensitic transformation characteristics of NiTiHf shape memory alloys. *Scr Mater*. <https://doi.org/10.1016/j.scriptamat.2018.10.008>
42. Scirè Mammano G, Dragoni E (2015) Effect of stress, heating rate, and degree of transformation on the functional fatigue of Ni-Ti shape memory wires. *J Mater Eng Perform*. <https://doi.org/10.1007/s11665-015-1561-7>
43. Bertacchini OW, Lagoudas DC, Patoor E (2009) Thermomechanical transformation fatigue of TiNiCu SMA actuators under a corrosive environment – Part I: Experimental results. *Int J Fatigue*. <https://doi.org/10.1016/j.ijfatigue.2009.04.012>
44. Lagoudas DC, Miller DA, Rong L, Kumar PK (2009) Thermo-mechanical fatigue of shape memory alloys. *Smart Mater Struct*. <https://doi.org/10.1088/0964-1726/18/8/085021>
45. Karhu M, Lindroos T (2010) Long-term behaviour of binary Ti–49.7Ni (at.%) SMA actuators—the fatigue lives and evolution of strains on thermal cycling. *Smart Mater Struct*. <https://doi.org/10.1088/0964-1726/19/11/115019>
46. Tugrul HO, Saygili HH, Kockar B (2020) Influence of limiting the actuation strain on the functional fatigue behavior of Ni_{50.3}Ti_{29.7}Hf₂₀ high temperature shape memory alloy. *J Intell Mater Syst Struct*. <https://doi.org/10.1177/1045389x20953610>
47. Ganesan S, Vedamanickam S (2022) Effect of operating parameters on functional fatigue characteristics of an Ni-Ti shape memory alloy on partial thermomechanical cycling. *J Intell Mater Syst Struct*. <https://doi.org/10.1177/1045389x211072233>
48. Akgul O, Tugrul HO, Kockar B (2020) Effect of the cooling rate on the thermal and thermomechanical behavior of NiTiHf high-temperature shape memory alloy. *J Mater Res*. <https://doi.org/10.1557/jmr.2020.139>
49. Karakoc O, Hayrettin C, Bass M, Wang SJ, Canadinc D, Mabe JH, Lagoudas DC, Karaman I (2017) Effects of upper cycle temperature on the actuation fatigue response of NiTiHf high temperature shape memory alloys. *Acta Mater* 138:185–197
50. Padula S, Qiu S, Gaydos D, Noebe R, Bigelow G, Garg A, Vaidyanathan R (2012) Effect of upper-cycle temperature on the

- load-biased, strain-temperature response of NiTi. *Metall Mater Trans A* 43(12):4610–4621
51. Clingman DJ, Calkins FT, Smith JP: Thermomechanical properties of Ni 60% weight Ti 40% weight. In: *Smart structures and materials 2003: active materials: behavior and mechanics*, vol 5053. SPIE, pp 219–229 (2003)
 52. Grossmann C, Frenzel J, Sampath V, Depka T, Eggeler G (2009) Elementary transformation and deformation processes and the cyclic stability of NiTi and NiTiCu shape memory spring actuators. *Metall Mater Trans A* 40(11):2530
 53. Karakoc O, Atli KC, Benafan O, Noebe RD, Karaman I (2022) Actuation fatigue performance of NiTiZr and comparison to NiTiHf high temperature shape memory alloys. *Mater Sci Eng A* 829:142154
 54. Atli KC, Karaman I, Noebe RD (2011) Work output of the two-way shape memory effect in $Ti_{50.5}Ni_{24.5}Pd_{25}$ high-temperature shape memory alloy. *Scr Mater* 65(10):903–906
 55. Scirè Mammano G, Dragoni E (2014) Functional fatigue of Ni–Ti shape memory wires under various loading conditions. *Int J Fatigue* 69:71–83
 56. Jardine AP, Bartley-Cho JD, Flanagan JS (1999) Improved design and performance of the SMA torque tube for the DARPA Smart Wing Program. In: *Smart structures and materials 1999: industrial and commercial applications of smart structures technologies*, vol 3674. SPIE, pp 260–269
 57. Mabe JH, Ruggeri RT, Rosenzweig E, Yu CJM (2004) NiTiInol performance characterization and rotary actuator design. In: *Smart structures and materials 2004: industrial and commercial applications of smart structures technologies*, vol 5388. SPIE, pp 95–109
 58. Benafan O, Gaydos DJ (2018) Constant-torque thermal cycling and two-way shape memory effect in $Ni_{50.3}Ti_{29.7}Hf_{20}$ torque tubes. *Smart Mater Struct* 27(7):075035
 59. Nicholson DE, Bass MA, Mabe JH, Benafan O, Padula SA, Vaidyanathan R (2016) Heating and loading paths to optimize the performance of trained shape memory alloy torsional actuators. In: *Smart materials, adaptive structures and intelligent systems*, vol 50480. American Society of Mechanical Engineers, p V001T02A008
 60. Stroud H, Hartl D (2020) Shape memory alloy torsional actuators: a review of applications, experimental investigations, modeling, and design. *Smart Mater Struct* 29(11):113001
 61. Nicholson DE, Padula SA, Benafan O, Bunn JR, Payzant EA, An K, Penumadu D, Vaidyanathan R (2021) Mapping of texture and phase fractions in heterogeneous stress states during multiaxial loading of biomedical superelastic NiTi. *Adv Mater* 33(5):2005092

Publisher's Note Springer Nature remains neutral with regard to jurisdictional claims in published maps and institutional affiliations.

Springer Nature or its licensor (e.g. a society or other partner) holds exclusive rights to this article under a publishing agreement with the author(s) or other rightsholder(s); author self-archiving of the accepted manuscript version of this article is solely governed by the terms of such publishing agreement and applicable law.